#6164

TURBULENCE MODELLING CHALLENGES POSED BY COMPLEX FLOWS

M A Leschziner
UMIST, Mechanical Engineering Department,
P.O. Box 88, Manchester

ABSTRACT

The paper discusses some influential issues pertaining to the computational modelling of multi-dimensional, separated, turbulent flow. The first part considers, mostly in qualitative terms, the modelling implications of a range of distinct physical flow characteristics. Issues addressed here include the interaction between turbulence, streamline curvature, buoyancy and normal strain, and the relevance of adverse pressure gradient, acceleration, separation and three-dimensionality. Attention is then focused on modern approaches to turbulence modelling, based mainly on second-moment closure and including adaptations to low-Reynolds-number regions. Established model variants are introduced and recent developments are reviewed, with a number of application examples included to support the discussion.

SOME INFLUENTIAL FLOW FEATURES AND RELATED ISSUES

What is Simple and What is Complex?

Complexity, like beauty, is in the eye of the beholder. To the aerodynamicist, the flow around an entire aircraft is complex; to the turbulence modeller, a curved two-dimensional boundary layer, a weak wake or a thermally driven flat-plate boundary layer are complex. The essential point of difference is turbulence, and the fact that its consequences must, in a practical context, be captured by a flimsy bridge spanning the deep gorge separating physical reality from industrial needs and constraints.

To start with, any boundary layer, be it plane or curved, is characterised by a high level of turbulence anisotropy, strong viscous/turbulence interaction in the immediate vicinity of the wall, and intermittency at its outer edge. The fact that such a complex amalgam can be computed by some very simple algebraic models is a consequence of some fortunate physical facts, combined with a pragmatic approach to modelling. Thus, transport of turbulence is rather weak in a boundary layer, unless the layer is severely accelerated or decelerated; the normal Reynolds stresses do not contribute measurably to the mean-momentum balance, which is dictated by the shear stress alone; the damping of turbulence as the wall is approached, whilst closely associated with the tendency towards two-dimensional turbulence, can be (and usually is) 'correlated' to a turbulent Reynolds number of the form $R_t=k^{0.5}\ell/\nu$, in which ℓ is either the distance from the wall or the length scale $k^{1.5}/\varepsilon$. This approach to characterising turbulence damping implies, of course, that the process is primarily induced by viscosity. In fact, it is provoked, principally, by an inviscid mechanism which selectively inhibits the wall-normal intensity via an interaction of wall-reflected pressure fluctuations and strain fluctuations. The consequence of this attenuation emerges from the (exact) production rate of the shear stress for homogenous shear:

$$P_{uv} = -\overline{v^2}\,\frac{\partial U}{\partial y} \tag{1}$$

To a first approximation, the shear stress may be assumed to be proportional the rate of its production multiplied by a time scale (the banking analogy being *wealth=interest rate x time*), that is:

$$-\overline{uv} \;\alpha\; \overline{v^2}\,\frac{\partial U}{\partial y} \cdot \left[\frac{k}{\epsilon}\right] \tag{2}$$

which brings out the central role of the normal stress $\overline{v^2}$. The main implication of the above comments is that any turbulence model which is to represent realistically the near-wall decay of turbulence must resolve anisotropy and cannot be based on the eddy-viscosity concept.

Starting from the (less than) simple flat-plate boundary considered above, one may proceed to identify a hierarchy of complicating features which pose strong challenges to efforts directed towards the construction of general turbulence-modelling strategies. Such features include curvature, buoyancy, acceleration/deceleration, separation, reattachment/impingement and three-dimensionality. All are highly relevant to room-ventilation, as indeed they are to many other fluid-flow areas. Some of these features are considered in the following sub-sections.

Small Causes... Large Effects

The addition of even weak secondary strains or body forces to a shear layer can have surprisingly profound consequences apertaining to the structure of turbulence, implying the need for a high level of modelling sophistication. Streamline curvature, Fig. 1(a), is a case in point.

It is instructive to note first that inclusion of curvature leads to the (exact) shear-stress production rate:

$$P_{uv} = -\overline{v^2}\,\frac{\partial U}{\partial y} - \overline{u^2}\,\frac{\partial V}{\partial x} \tag{3}$$

In a wall boundary layer, $\overline{u^2}$ is much larger than $\overline{v^2}$. It is evident, therefore, that the curvature-related secondary strain, $\partial V/\partial x$, is heavily weighted relative to the principal strain and will, therefore, have a disproportionately large influence on the shear stress. The influence of curvature is further brought out by considering the exact production rates of the normal and shear stresses, expressed in terms of curved, streamline-adapted co-ordinates:

$$
\begin{aligned}
P_{\overline{uu}} &= -2\,\overline{uv}\left[\frac{\partial U}{\partial r} + \frac{U}{R}\right] \\
P_{\overline{vv}} &= 4\,\overline{uv}\,\frac{U}{R} \\
P_{\overline{uv}} &= -\,\overline{v^2}\,\frac{\partial U}{\partial r} + \left\{\left[2\,\overline{u^2}-\overline{v^2}\right]\frac{U}{R}\right\}
\end{aligned}
\tag{4}
$$

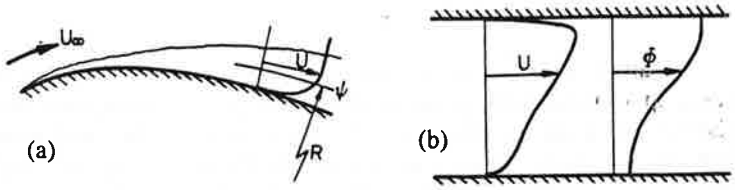

Fig. 1: Generic shear flows with curvature and density stratification

A number of useful qualitative observations may be made by reference to the above equations. It is noted first that the secondary strain U/R tends to increase $P_{\overline{uv}}$ and hence uv itself, since $2\overline{u^2}$ typically exceeds $\overline{v^2}$ by a factor 3. This stress is negative, however, and curvature will, consequently, reduce the magnitude of uv. Second, the influence of U/R is much stronger than one might expect, for its multiplier in $P_{\overline{uv}}$ is $(2\overline{u^2}-\overline{v^2})$ which is much larger than $\overline{v^2}$, the multiplier of the primary strain. That $\overline{v^2}$ is relatively small follows from the observation that $P_{\overline{uv}}$ is not simply low but is, in fact, negative. Of course, despite the negative production, $\overline{v^2}$ cannot itself be negative, and this is ensured by so-called "pressure-strain-interaction" processes which continuously 'feed' energy from $\overline{u^2}$ to $\overline{v^2}$. The stress $\overline{u^2}$ can well afford this loss, for it is generated at a high rate due to the interaction between uv and the primary strain $\partial U/\partial r$. The final point to note here is that the curvature-induced reduction in $\overline{v^2}$ leads to a further reduction in the magnitude of $\overline{uv}$ through the product of $\overline{v^2}$ and the primary strain in $P_{\overline{uv}}$. It is thus evident that curvature selectively attenuates $\overline{v^2}$ (but slightly increases $\overline{u^2}$), leading to a substantial reduction in $\overline{uv}$. In addition, uv is reduced directly by U/R.

Similar arguments apply to other curved or swirling flows in which turbulence may either be attenuated or amplified depending upon the sense of curvature. Equivalent consideration may also be made in relation to density-stratified flows, as is demonstrated in the example below. It is here that the well-known analogy emerges between curvature- and stratification-induced amplification or attenuation of turbulence. For the stratified and sheared flow in Fig. 1(b), the production rates of the stresses $\overline{v^2}$ and $\overline{uv}$ and the vertical flux $\overline{v\phi}$ are given by:

$$
\begin{aligned}
P_{\overline{uv}} &= -\overline{v^2}\,\frac{\partial U}{\partial y} + (\beta g\overline{v\varphi}) \\
P_{\overline{v^2}} &= 2g\beta\overline{v\varphi} \\
P_{\overline{v\varphi}} &= -\overline{v^2}\,\frac{\partial \Phi}{\partial y} + \left(\beta g\overline{\varphi^2} - \overline{v\varphi}\,\frac{\partial U}{\partial y}\right)
\end{aligned}
\tag{5}
$$

where $\beta=-1/\rho(\partial\rho/\partial\Phi)$ is the volumetric expansion coefficient. Here, the buoyancy-related production terms appearing in the $\overline{v^2}$-equation play the key role in determining the interaction between buoyancy, the stress uv and the principal flux $\overline{v\phi}$. Stable density stratification implies $\partial\Phi/\partial y>0$, and it follows that an increase in $\overline{v^2}$ results in a reduction in $P_{\overline{v\phi}}$ and hence $\overline{v\phi}$, which then lowers $\overline{v^2}$ and hence $P_{\overline{v^2}}$ (the latter being negative here). This, in turn, reduces the magnitude of $P_{\overline{uv}}$ and hence $\overline{uv}$. An analogous line of arguments may be applied to unstable stratification to show that, in that case, $\overline{v^2}$, $\overline{uv}$ and $\overline{v\phi}$ tend to increase.

The above considerations demonstrate that any serious attempt to represent realistically the physical processes at play in the presence of curvature, recirculation, swirl and body forces must rest on capturing turbulence anisotropy and its interaction with turbulence transport. They also clarify that many situations which superficially appear simple are, in fact, physically very complex. The large majority of room-ventilation problems are, of course, characterised by highly curved shear layers, recirculation regions, and stratified zones. Hence, the foregoing argument are highly relevant in the present context.

More speed.... Less Haste

The acceleration of a boundary layer, if sustained, is known to cause relaminarisation. Conversely, deceleration tends to increase turbulence, but the associated causes are not identical. Both may arise from streamwise pressure gradients and - of particular relevance to room ventilation - from streamwise-directed buoyancy forces, for example at a heated wall[1]. The origin of relaminarisation is ill-understood, but is believed to be connected to the suppression of turbulent spots generated by shear at the wall, from which turbulence emanates and propagates into the boundary layer (Kline et al [1]). A statistical concept of the process rests on the notion that the turbulent contribution to the total shear stress is partially 'frozen' due to convection, while the total shear stress must increase due to the increase in shear strain. Hence, the laminar contribution to the total shear stress tends to gain in importance and this leads to a sustained thickening of the semi-viscous sub-layer, coupled with a uniformisation of the outer stream and hence decline in shear-induced turbulence production. How this process interacts with anisotropy is unclear, but the considerations presented in the previous sub-section clearly imply that anisotropy must play an important role. Indeed, heat-transfer calculations in thermally-driven cavities derive considerable benefits from the use of the "generalised gradient-diffusion hypothesis" for the heat fluxes, which accounts for stress anisotropy (Ince & Launder [2]).

In the absence of any clear insight into the physical mechanism governing

---

[1] In fact, in mixed convection, wall-induced heating can result in both a reduction and an enhancement of turbulence, and consequently heat transfer. The crucial issue is the relative direction and magnitude of forced and free convection. For details see Cotton and Jackson [4].

relaminarisation, modelling research has tended to progress pragmatically along the route of 'simulating' the decay of viscous transport during acceleration by means of eddy-viscosity models which damp near-wall turbulence transport by diminishing the turbulence energy and, via the viscosity, the shear stress. The minimum closure level required to capture aspects of relaminarisation is a two-equation formulation in which transport equations are solved for a turbulent-velocity scale and a length scale. There are some 15 two-equation eddy-viscosity models documented in the literature (for a review of some, see Patel et al [3]), which all aim to account for low-Reynolds-number effects near the wall and acceleration effects. Their performance is very variable - as is demonstrated, for example, by Kawamura [5], and all rest on rather shaky ground. Very recent efforts address the question of the interaction between anisotropy and low-Re near-wall turbulence by way of advanced second-moment closures (Iacovides [6], Launder & Tselepidakis [7]); related progress will be indicated in a separate section to follow.

When a boundary layer is subjected to severe deceleration, the streamwise and lateral normal strains contribute significantly to the production rates of stresses. These former are pre-multiplied by the latter, and it follows, therefore, that a resolution of anisotropy can be important if the structure of the boundary layer is to be resolved adequately. This is likely to be of particular relevance in boundary layers heading towards separation from a continuously curved wall, rather than from a step or corner, for the point of separation will depend sensitively on the structure of the boundary layer just prior to separation. A curious physical feature of a decelerating boundary layer that the turbulent length scale appears to quite insensitive to the rate of deceleration, maintaining a value very close to the equilibrium level (ℓ=0.42y in terms of the mixing-length concept). This, present models are unable to represent; all yield excessive values, and *ad-hoc* corrections, identified later, are needed to depress the length-scale level.

Hitting a Brick Wall

When an irrotational, but turbulent stream impinges normally on a wall, turbulence tends to be generated by normal straining. However, the rate of generation is much lower than might be supposed. This may be clarified by reference to the exact generation rate of turbulence energy:

$$P_k = -\rho\overline{uu}\frac{\partial U}{\partial x} - \rho\overline{vv}\frac{\partial V}{\partial y} - \rho\overline{uv}\left[\frac{\partial U}{\partial y} + \frac{\partial V}{\partial x}\right] \tag{6}$$

Near the stagnation point, the first two terms dominate P_k. Because the divergence of the flow is zero, the first and second terms partially cancel each other. To what extent, depends strongly on the level of normal-stress anisotropy. Here again, anisotropy plays a crucial role. More importantly, if the eddy-viscosity hypothesis is used in conjunction with the Boussinesq stress-strain relations, the above production rate becomes:

$$P_k = 2\mu_t\left[\frac{\partial U}{\partial x}\right]^2 + 2\mu_t\left[\frac{\partial V}{\partial y}\right]^2 + \mu_t\left[\frac{\partial U}{\partial y} + \frac{\partial V}{\partial x}\right]^2 \tag{7}$$

which yields a seriously excessive level.

A different type of impingement occurs at a reattachment point following separation (say, behind a backward-facing step). This impingement is not only oblique, but involves the transport of highly strained and highly turbulent fluid towards the wall. Here, wall-induced turbulence damping, due to the influence of wall-induced pressure-reflection on anisotropy, is highly influential and must be represented realistically if the point of reattachment, and hence the size of the recirculation zone are to be determined accurately. This is a major challenge to established forms of second-moment closure which show prominent weaknesses in respect of reattachment. Some recent progress in this area will be reported later.

Facing Three-Dimensional Reality

The large majority of flows are three-dimensional, and this poses a number of additional challenges, both in relation to numerical and turbulence-modelling issues. As regards the latter, one consequence is a that the number of active stresses, interacting with strains, rises from 3 to 6. Turbulence models, of whatever complexion, are almost invariably constructed and 'calibrated' by reference to selected two-dimensional flows. Hence, in 3D, these models are used in an extrapolatory mode, and any (numerate) scientist will be acutely aware of the fallibility of any extrapolation scheme.

Another problem peculiar to three-dimensional flow is the skewness of the velocity relative to the wall, arising from transverse secondary motion superimposed on the primary component. This is best exemplified by the conditions encountered in a curved duct - say one used for ventilation. Because of the duct's curvature (which itself will significantly affect the turbulence structure), there arises a transverse secondary motion (of the "first kind"). Typically, the maximum velocity of this motion is 20-40% of the primary component. More importantly, the maximum lies very close to the wall, often within the viscous sublayer. This has two important implications: first, the wall-parallel component of the velocity vector changes its orientation at a high rate as the wall is approached. Hence, an accurate and detailed resolution of the transverse motion, which governs the important convective redistribution of streamwise momentum, is essential. In others words, a log-law based computational bridge across the sublayer, often used to save resources, is likely to be erroneous. Second, in contrast to a 2D boundary layer, Reynolds-stress transport in a 3D layer contributes significantly to the stress balance. Hence, it is likely that modelling at second-moment level will have to include stress transport to yield a realistic prediction of the near-wall structure.

What about Organised Transient Features?

While any turbulent flow is inherently unsteady, this unsteadiness is disorganised and aperiodic. There are many circumstances, however, in which large-scale periodic features coexist with essentially random turbulence. Examples are Vortex-shedding behind bluff bodies, Rayleigh-Benard convection and Taylor vortices in rotating flows. There is no reason to assume that the effects of these structures is accounted for correctly within the statistical modelling framework. Indeed, in the case of vortex shedding, there is a range of evidence to suggest that turbulence models yielding steady-state solutions underestimate the apparent mixing implied by an *a-posteriori* time-averaging of the transient solution derived from a simulation which resolves at least the large-scale structures shed from the bluff obstacle. An associated problem is that different turbulence models suppress to a variable extent naturally occurring periodicity. Fig. 2 gives an example from mechanical engineering (Lin and Leschziner [8]). Here, a jet is issued from a radial injector into a swirling cross-flow. The interaction between the two flows produces a periodic flapping motion associated with shedding. The flow was computed with two models: an eddy-viscosity k-ε variant and a Reynolds-stress-transport closure. The latter tends to return a lower level of turbulence mixing resulting in a more pronounced flapping mode. This is brought out in Fig. 2 by a comparison of frequency spectra obtained by a Fourier analysis. Evidently, different model variants include different time-scale ranges, suggesting an overlap between turbulence and shedding time scales. In extreme cases (Franke et al [9]), the turbulence model entirely suppresses any transients and returns a steady solution which does not conform with the real time-averaged behaviour. It must be said here that the above difficulty is encountered predominantly in unconfined conditions. Confinement and wall proximity tend to inhibit periodicity and enhance the validity of the statistical framework.

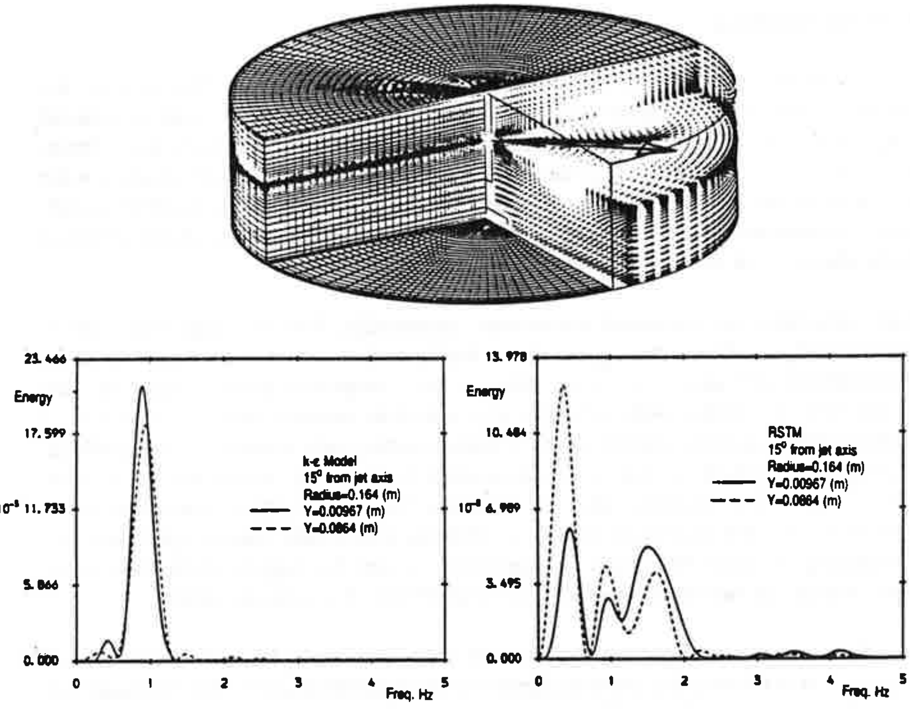

Fig. 2: Jet injected into cross flow and flapping frequency spectra predicted by k-ε eddy-viscosity model and Reynolds-stress transport model (Lin & Leschziner [8])

In the event of extrema (say, peak velocity and heat transfer) having to be determined, a statistical framework is obviously inappropriate, although some very limited information can be derived from the predicted (steady) correlations of turbulent fluctuations. In this case, the only alternative route is Large Eddy Simulation. This approach, vigorously pursued in Japan and the USA (Tamura et al [10], Murakami et al [11], Reynolds [12]), resolves scales down to the size of the (relatively coarse) grid and accounts for smaller scales by way of a sub-grid model, the nature of which is similar to conventional statistical models of turbulence. While this route avoids the difficulties pointed out earlier, it has its weaknesses: it is especially costly; it requires the use of particularly accurate approximation techniques which tend to instability in high Reynolds-number flow; it entails the storage of large quantities of data in the form of time series, from which statistical information needs to be extracted by integration after time-marching is completed; it requires the prescription of transient boundary conditions which are not available but must be generated numerically; and it involves serious uncertainties relating to semi-viscous near-wall effects and their simulation. This paper is does not consider LES further, but confines itself to issues relevant to the computation of flows with turbulence models.

A Word on Numerics

For computational solutions to reflect reality and to give a fair representation the predictive capabilities of the turbulence closures used, numerical errors must be reduced to insignificant levels. This is an especially difficult task in highly convective, three-dimensional recirculating flow, and the problem may be seriously compounded by the need to resolve the semi-viscous sublayer by way of a low-Reynolds-number model. Moreover, computations with advanced second-moment closure are particularly sensitive to errors arising from artificial diffusion, and require great care.

In most circumstances, numerical errors arise, principally, from the approximation of convective transport. Convection gives rise to highly strained (compressed and sheared), often convoluted regions and steep variations in flow properties. If these variations are to be resolved accurately with economically tolerable meshes, convection must be approximated with higher-order numerical schemes, particularly when the steep gradients are significantly skewed relative to the numerical mesh - as is invariably the case in complex flows. The problem here is, however, that such approximations tend to provoke instability and oscillatory solutions - features which have discouraged their use. The frequently adopted alternative is, therefore, to opt for highly stable low-order schemes, which can introduce unacceptably high levels of numerical error.

Numerical errors are brought out particularly well by simple tests in which a uni-directional flow is deliberately skewed relative to the supporting grid. Two examples are shown in Figs. 3 and 4. In the former, reported by Leschziner [57], a plane laminar jet is discharged at 22.6^{o} relative to the horizontal, with the maximum cell-Peclet number ($V\Delta x/\nu$) being 50. Its development is resolved with three convection schemes: the first-order upwind scheme, a skew-upwind variant (Raithby [13]) in which (first-order) upwinding is effected in the streamwise direction, and the third-order upstream-weighted quadratic interpolation scheme QUICK (Leonard [14]). While none of the schemes returns close agreement with the exact solution, the first-order upwind approximation gives a wholly unacceptable level of artificial smearing which renders the related solution meaningless. Unfortunately, this scheme is still widely used in multidimensional flow simulations, including such related to room-ventilation (e.g Davidson [15]).

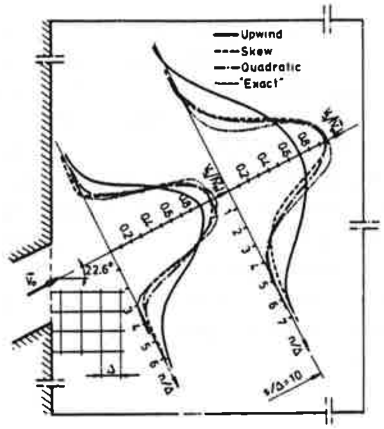

Fig. 3: Laminar plane jet discharged at 22.6° to grid - comparison of predictions with exact solution for Pe_x=50 (Leschziner [57])

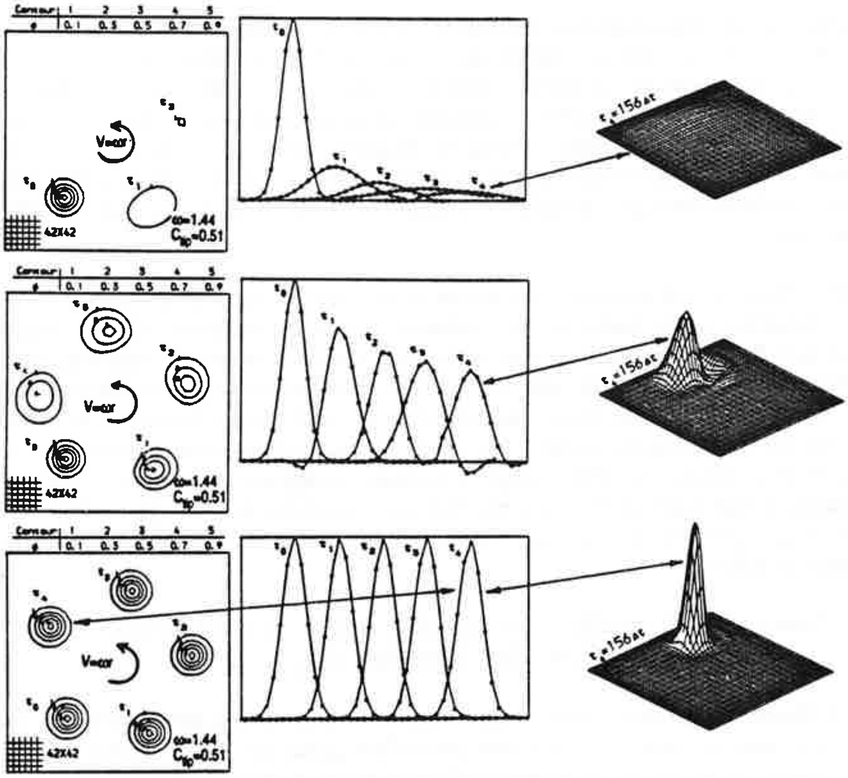

Fig. 4: Convective transport of Gaussian scalar field by a forced vortex at tip Courant number C_{tip}=0.5; (a) 1st-order Upwind/ADI scheme; (b) QUICK/ADI scheme, (c) Spline/Characteristics scheme (Nasser [13])

Fig. 4 relates to a time-dependent case, and compares numerical solutions, arising from three different convection approximations, for the purely convective transport of a Gaussian-shaped conserved scalar by a forced vortex (solid-body rotation). Solutions 4(a) and 4(b) have been obtained with the first-order upwind approximation and the quadratic scheme QUICK, respectively, both combined with a second-order ADI time-marching method. Solution 4(c) was generated with a spatially fourth-order spline approximation combined with a time-space characteristics method (Nasser [16]). As seen, the upwind scheme returns a very rapid artificial decay and is effectively worthless. Although the QUICK scheme is generally assumed to be quite accurate and is widely used, it is evident that it too results in serious artificial erosion of the scalar distribution. Only the third, most elaborate scheme is here able to maintain a high level of accuracy.

SOME CURRENT DIRECTIONS IN TURBULENCE MODELLING

Second-moment closure

As stated earlier, eddy-viscosity models are not able to represent the sensitivity of turbulence to rotation, curvature and body forces. A highly over-simplified (and partial) explanation of this failure is that the isotropic nature of the eddy viscosity does not permit the strong curvature/buoyancy-induced enhancement of normal-stress anisotropy to be captured. This anisotropy, created by different levels of stress generation and turbulence-energy redistribution among the normal stresses, then feeds into the shear stresses and fluxes through a complex interaction between all the stress, flux and strain components.

The lowest level of turbulence closure which offers a real prospect of accounting for the above interaction is one based on the solution of separate equations for all independent stresses and fluxes. This route is now well established and taken in computing many complex flows, featuring *inter alia* recirculation, swirl, compressibility, large density variations, combustion and three-dimensionality [17,18]. Exact forms of the stress equations can be obtained by lengthy, but otherwise straightforward manipulations of the Navier-Stokes, Reynolds and energy equations. Adopting a simple descriptive representation and denoting the stress and flux components by $\overline{u_i u_j}$ and $\overline{u_i \phi}$, respectively, (where i=1,2,3 relate to the x,y,z directions), one may write the resulting stress or flux equations as follows:

$$\text{Convection } (\overline{u_i u_j} \text{ or } \overline{u_i \phi}) = \text{Diffusion } (\overline{u_i u_j} \text{ or } \overline{u_i \phi}) + \text{Production } (\overline{u_i u_j} \text{ or } \overline{u_i \phi})$$
$$+\text{Redistribution } (\overline{u_i u_j} \text{ or } \overline{u_i \phi}) - \text{Dissipation } (\overline{u_i u_j} \text{ or } \overline{u_i \phi})$$

While diffusion, redistribution and dissipation all require modelling, production does not, for it only involves stresses, fluxes and mean-flow gradients. As the stress and flux levels respond sensitively to the related production levels, it can be concluded tentatively that a model based on the above principles offers a superior range of generality.

The most commonly used Reynolds-stress closure form is that of Gibson & Launder

[19] (based on that of Launder et al [20]). This consists of the following modelled transport equations for the stresses $\overline{u_i u_j}$:

$$\underbrace{\frac{\partial U_k \overline{u_i u_j}}{\partial x_k}}_{C_{ij}} = \underbrace{\frac{\partial}{\partial x_k} C_s \overline{u_k u_\ell} \frac{k}{\epsilon} \frac{\partial \overline{u_i u_j}}{\partial x_\ell}}_{d_{ij}} + P_{ij} + \Phi_{ij} - \frac{2}{3} \delta_{ij} \epsilon \tag{8}$$

where U_k are mean-velocity components in the directions x_k;

$$P_{ij} \equiv - \overline{u_i u_k} \frac{\partial U_j}{\partial x_k} + \overline{u_j u_k} \frac{\partial U_i}{\partial x_k} \tag{9}$$

is the generation of the stress $\overline{u_i u_j}$, Φ_{ij} controls the re-distribution of turbulence energy, $k = \overline{u_k u_k}$, among the normal stresses, and $2/3\varepsilon\delta_{ij}$ stands for the rate of dissipation of the normal stresses by the action of viscosity. In the above, convection and generation are exact, while the remaining terms are models of exact expressions which cannot be used in their original form, however, as they contain third-order correlations. Thus, diffusion is modelled by a generalized gradient approximation, while dissipation is assumed to be isotropic, with each normal stress dissipated at the same rate, $2/3\varepsilon$, where ε is determined from its own transport equation,

$$\frac{\partial U_k \epsilon}{\partial x_k} = \frac{\partial}{\partial x_k} C_\epsilon \overline{u_k u_\ell} \frac{k}{\epsilon} \frac{\partial \epsilon}{\partial x_\ell} + C_{\epsilon,1} \frac{\epsilon}{2k} P_{kk} - C_{\epsilon,2} \frac{\epsilon^2}{k} \tag{10}$$

Finally, the redistribution term, Φ_{ij}, modelling the interaction between turbulent fluctuations of pressure and strains, consists of three contributions, namely Rotta's linear 'return to isotropy' term,

$$\Phi_{ij,1} = - \frac{C_1 \epsilon}{k} \overline{u_i u_j} - \frac{1}{3} \delta_{ij} \overline{u_k u_k} \tag{11}$$

the 'isotropization of production' term,

$$\Phi_{ij,2} = - C_2 \; P_{ij} - \frac{1}{3} \delta_{ij} P_{kk} \tag{12}$$

and the 'wall-reflection' terms,

$$\begin{aligned} \Phi^w_{ij,1} &= C_{1,w} \frac{\epsilon}{k} (\overline{u_k u_m} n_k n_m \delta_{ij} - \frac{3}{2} \overline{u_k u_i} n_k n_j - \frac{3}{2} \overline{u_k u_j} n_k n_i) \, f \\ \Phi^w_{ij,2} &= C_{2,w} (\Phi_{km,2} n_k n_m \delta_{ij} - \frac{3}{2} \Phi_{ik,2} n_k n_j - \frac{3}{2} \Phi_{jk,2} n_k n_i) \, f \end{aligned} \tag{13}$$

The above is a particular form expressing only the influence of the nearest wall via the wall distance function

$$f = \frac{k^{1.5}}{2.5\epsilon} \; \frac{1}{r} \tag{14}$$

ζ being the distance from the wall. A simplified form of the above closure is the so-called algebraic stress model (ASM). Its derivation was (misguidedly) motivated by considerations of computational economy. It arises upon the replacement of the differential stress-convection and diffusion terms, for example, by Rodi's proposal [21],

$$(C_{ij} - d_{ij}) \rightarrow \frac{\overline{u_i u_j}}{k} (C - d) = \frac{\overline{u_i u_j}}{k} (P - \epsilon) \qquad (15)$$

where C, d, P and ε represent convection, diffusion, production and dissipation of turbulence energy, respectively. The essential feature to note here is that, once k and ε (and hence P) have been determined from the related differential equations, equations (8), incorporating the model (15), inter-relate the stresses algebraically. The ASM, although often used, is known to display weaknesses in a number of circumstances, particularly in the presence of swirl. Quite generally, the algebraic transformation is neither co-ordinate invariant nor does it give a satisfactory approximation of the transport of *shear stresses* (Fu et al [22]). Hence, the parent form (8) is always preferable.

Much work has been done, especially over the past seven years, on the validation of the above forms and related variants by reference to complex flows [18]. At UMIST alone, some twenty recirculating and strongly swirling flows have been examined, among them three-dimensional and transonic flows. Just four purely aerodynamic examples are included here to convey an impression of the performance of second-moment closure relative to that of the k-ε eddy-viscosity model.

Fig. 5 relates to a jet injected into a plenum chamber. The flow, examined experimentally by Boyle and Golay [23], is affected by three-dimensional features because of spanwise confinement. The computations, by Huang & Leschziner [24], are two-dimensional, however, and some caution is in order, therefore, when considering correspondence between computation and experiment. What the results in Fig. 5 are primarily intended to demonstrate is that streamline curvature in the shear layer bordering the recirculation zone dramatically attenuates viscous transport. The effect on the flow field is moderate, but turbulence energy is depressed by half an order of magnitude, with obvious implications relating to heat-transfer predictions.

Fig. 6 shows calculations for a separated flow over a curved, stepped centrebody suspended in an annular diffuser (Leschziner et al [25]). The upper streamfunction plot indicates that the stress closure (an algebraic variant in this case) returns a significantly larger recirculation zone that the eddy-viscosity model, due to its ability to capture curvature-induced turbulence attenuation in the separated shear layer. The lower pressure-recovery plots, relating to two axial locations of the centrebody within the diffuser, provide a clear indication that the stress closure also returned the correct *shape* of the recirculation zone, for pressure recovery is dictated by the effective flow area between the diffuser wall and the separation streamline. Very similar conclusions are derived from the application of the full transport closure. Thus Fig. 7 shows a comparison of partial streamfunction fields computed by Lien [26] for a flow behind a backward-facing step in a 6^o expanding channel measured by Driver & Seegmiller [27].

Here again, the critical issue is streamline curvature in the separated shear layer.

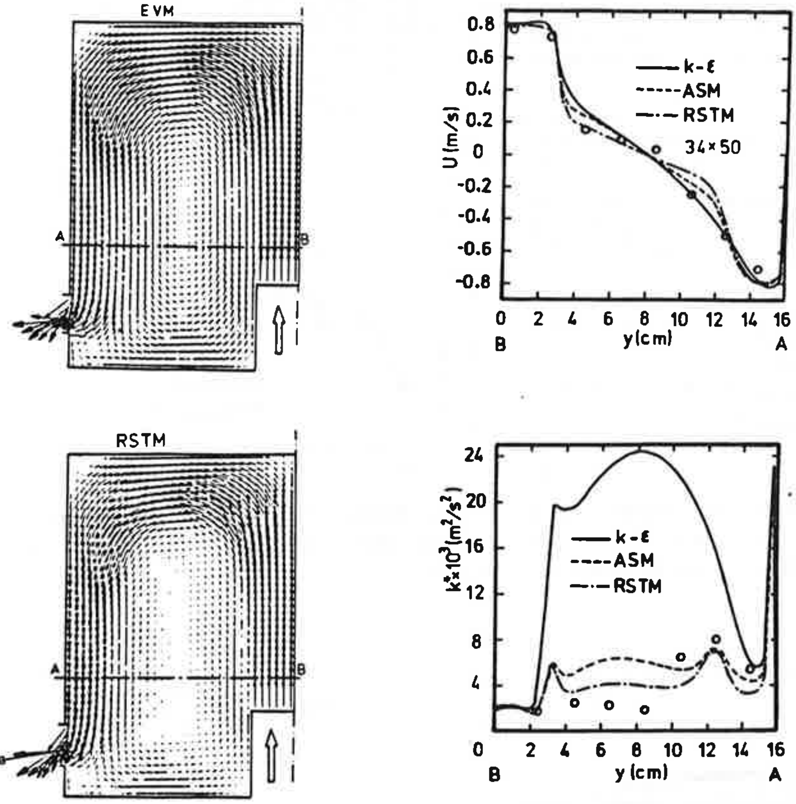

Fig. 5: Jet injection into a plenum chamber: velocity field and profiles of velocity and turbulence energy predicted with eddy-viscosity and Reynolds-stress models (Huang & Leschziner [24])

Finally, Fig. 8 relates to a three-dimensional twin-jet configuration (Saripalli [28]) in which impingement gives rise to a strong fountain originating from the collision of the wall jets formed after impingement. The greatest sensitivity to turbulence modelling is, not unexpectedly, observed in the fountain, and computational results by Ince & Leschziner [29] included here relate to the fountain half-width and cross-fountain velocity. As seen, the Reynolds-stress model yields a clearly superior resolution, held to reflect the destabilising influence of curvature in the near-wall shear layers which rise from the wall at the base of the fountain as the wall jets collide.

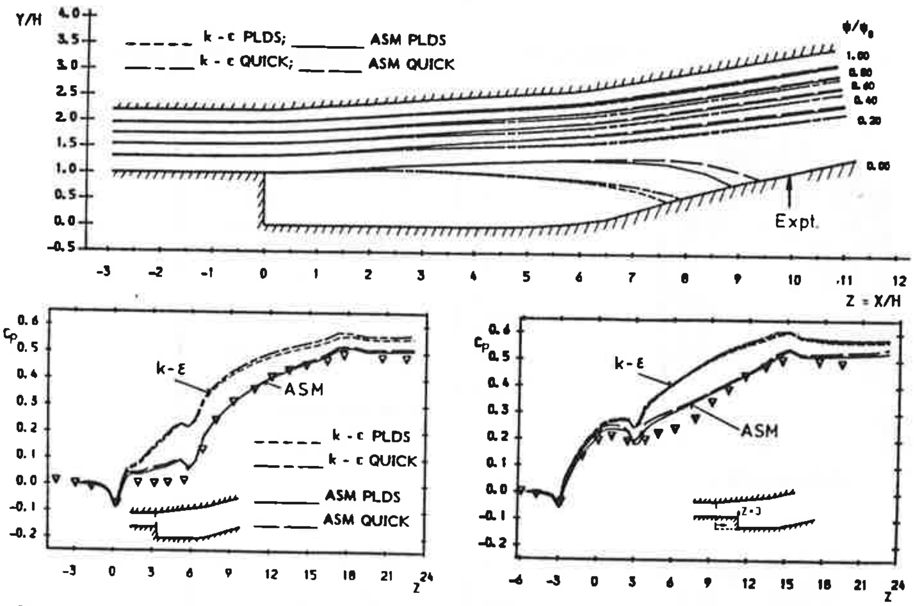

Fig. 6: Streamfunction and pressure recovery in separated flow in expanding annular passage: response to turbulence model and numerical approximation of convection scheme (Leschziner et al [25])

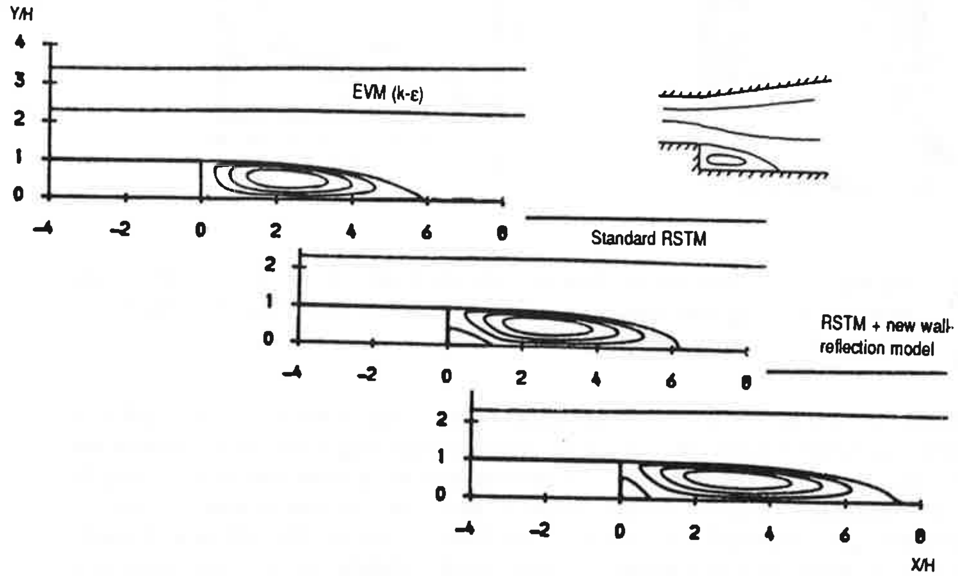

Fig. 7: Partial view of streamfunction field in 6° backward-facing-step flow predicted with eddy-viscosity and Reynolds-stress-transport models (Lien [26])

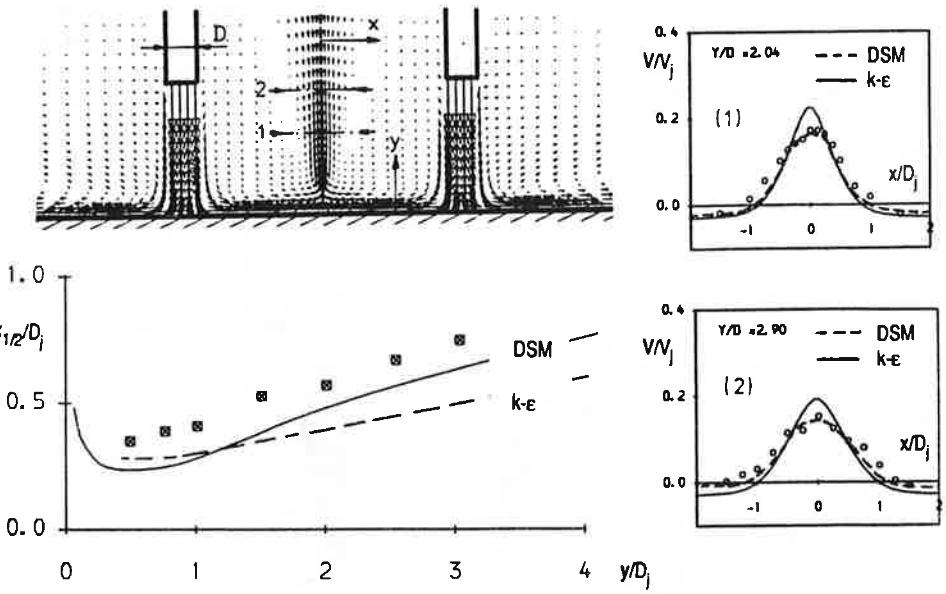

Fig. 8: Flow field, fountain half-width and fountain-velocity profiles in centre plane of twin-impinging jet computed with eddy-viscosity and Reynolds-stress-transport models (Ince & Leschziner [29])]

Space constraints do not permit a great deal to be said about the extension of the above framework to heat fluxes and on the performance of the extended model; attention is drawn, however, to comments made in the introductory section on some fundamental issues related to temperature stratification. The extension involves the inclusion of modelled equations for the fluxes themselves and, in general, of two further equations, one for the variance of the scalar quantity being considered (e.g. internal energy, temperature, species concentration) and one for the dissipation of this variance [19]. There is ample evidence to demonstrate that the extended closure and truncated variants thereof are able to represent the inhibiting/amplifying influence of stable/unstable density stratification on the vertical exchange of momentum and heat. Leschziner [30] and McGuirk et al [31] show, for example, that flux-model variants are able to predict internal hydraulic jumps resulting from the horizontal discharge of warm over cold water. Viollet [32] reports striking calculations for stably and unstably stratified water flows which verify the ability of second-moment closure to mimic damping and enhancement of vertical mixing. Further examples involving three-dimensional warm-water discharges into colder water bodies are reported by McGuirk & Rodi [33] and Leschziner & Rodi [34]. Results from a particularly demanding calculations by Cresswell et al [58] performed with two full Reynolds-stress-transport models for a negatively buoyant warm jet issuing into an opposing colder stream are shown in Fig. 9. Here, essential processes to capture are those arising from the strong interaction between turbulence, curvature and buoyancy. Plots included in Fig. 9 show the overall flow field and radial profiles of temperature, Reynolds-stresses, radial flux and temperature variance at one axial location. The essential point to highlight here is that all turbulence quantities, which are especially sensitive to curvature and buoyancy, have been well captured, particularly by closure-variant 2 which embodies cubic pressure-strain and pressure-temperature-gradient approximations (see later considerations). Any eddy-viscosity approach would entire fail to give a realistic description of the turbulence field in this case.

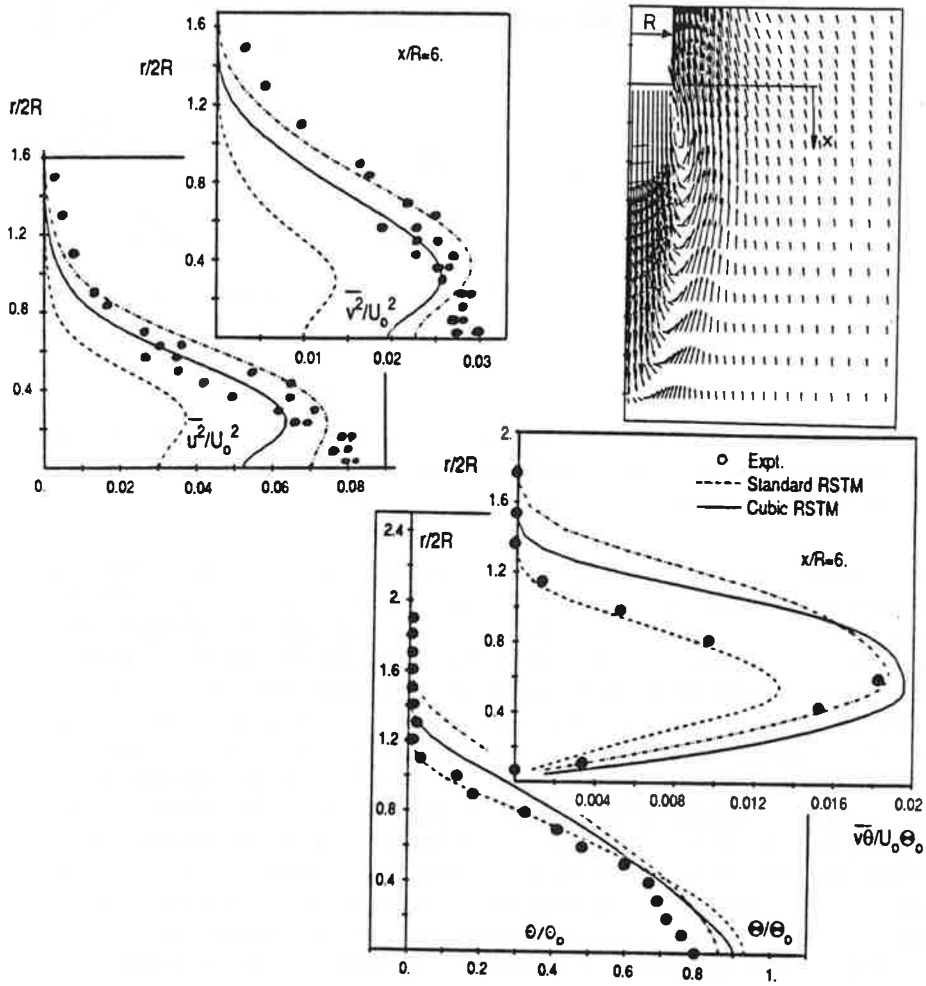

Fig. 9: Flow field and profiles of temperature, Reynolds stresses, lateral heat flux and temperature variance in negatively buoyant jet predicted with two Reynolds-stress-transport variants (Cresswell et al [58])

Notwithstanding the rather upbeat account given above, it must be acknowledged that the gains achieved by switching from an eddy-viscosity to a Reynolds-stress closure are not uniformly high, and the latter is by no means a panacea. Yet, no case has been encountered which has derived no benefit from the switch. Swirling flows and those dominated by large recirculating regions seem to benefit most, and this conclusion extends to three-dimensional conditions. Weaknesses in the forms used in the above examples are rooted, principally, in the approximation of the pressure-strain and the dissipation processes. The former acts against the anisotropy-provoking generation terms by redistributing energy among the normal stresses, simultaneously reducing the shear stresses. The standard model depends linearly on shear stresses, but there is every reason to believe that the dependence is non-linear. Indeed, the linear form is inherently unable to represent the decline of isotropisation as the wall is approached, where turbulence tends to become two-dimensional. It is this inability which necessitates the use of the highly intuitive, yet highly influential wall-reflection terms (13). Their task is, essentially, to counteract excessive isotropisation by models (11) and (12). The linear form is also known to give the wrong response in strong homogeneous shear where the production-to-dissipation ratio P_k/ε significantly exceeds 1.

Over the past four years, efforts have been made by groups around Lumley [35] and Launder [36] to construct non-linear pressure-strain models designed to satisfy the "realizability constraint":

$$\phi_{\alpha\alpha,2} \rightarrow 0 \quad \text{as} \quad u^2_{\alpha\alpha} \rightarrow 0 \tag{16}$$

(no summation on α which denotes direction of principal strains) and to minimise the need for wall-correction terms.

Thus, Fu et al [36], guided by earlier work of Shie and Lumley [35], have derived the following cubic model for the pressure-strain term $\phi_{ij,2}$

$$\begin{aligned}\phi_{ij2} = &- 0.6\,[P_{ij} - \tfrac{1}{3}\delta_{ij} P_{kk}] + 0.3\varepsilon a_{ij}\,(P_{kk}/\varepsilon)\\ &- 0.2\Big\{\frac{\overline{u_k u_j}\;\overline{u_\ell u_i}}{k}\Big[\frac{\partial U_k}{\partial x_\ell} + \frac{\partial U_\ell}{\partial x_k}\Big] - \frac{\overline{u_\ell u_k}}{k}\Big[\overline{u_i u_k}\frac{\partial U_j}{\partial x_\ell} + \overline{u_j u_k}\frac{\partial U_i}{\partial x_\ell}\Big]\Big\}\\ &- r\,[A_2\,(P_{ij} - D_{ij}) + 3a_{mi}\,a_{nj}\,(P_{mn} - D_{mn})]\end{aligned} \tag{17}$$

Which, together with the non-linear form for $\phi_{ij,1}$

$$\phi_{ij,1} = - C_1 \frac{\varepsilon}{k}\,[a_{ij} + C_1'(a_{ik}\,a_{kj} - \tfrac{1}{3}\delta_{ij} A_2)] - \varepsilon a_{ij} \tag{18}$$

ensures that ϕ_{nn}, and with it $\overline{u^2_{nn}}$ (n=wall-normal index), vanish at the wall. In the above, 'A' is (a highly influential) "flatness parameter" given by $A=\{1-9/8(A_2-A_3)\}$ where $A_2=a_{ij}a_{ij}$ is the second invariant of tha anisotropy $a_{ij}=(\overline{u_iu_j} - 2/3\ \delta_{ij}k)/k$ and $A_3=a_{ij}a_{jk}a_{ki}$ is the third invariant. The importance of 'A' derives from Lumley's observation that its value is unity for isotropic turbulence and zero for 2D turbulence.

The validation of the above model by reference to complex flows is in its infancy. The only extensive validation study documented to date is that of Craft [38], who examined the cubic model, in conjunction with a newly formulated pressure-reflection model (see later), in the case of a round jet impinging on a flat plate close to the jet. Velocity profiles predicted by the 'standard' and the cubic models across two streamwise jet locations are shown in Fig. 10. Although the cubic model is seen to perform well here, it must be added that at large h/D values the model, in its present form, returns excessive k-values leading to a deterioration in predictive quality. A better practice is to combine the linear model with Craft & Launder's [37] new wall-reflection model.

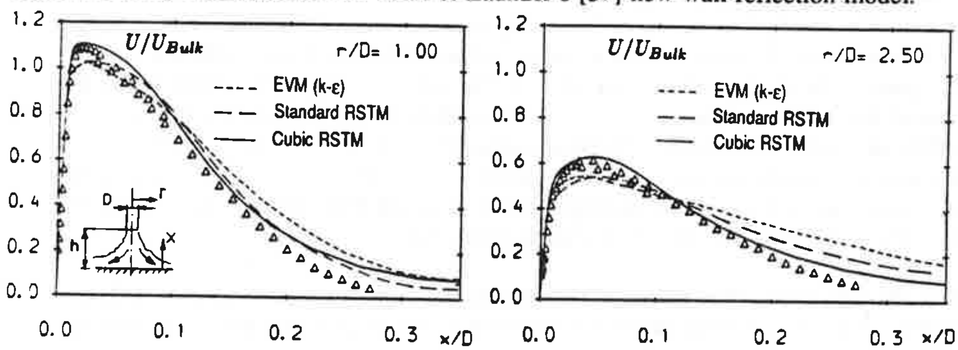

Fig. 10: Velocity profiles in round, normally-impinging jet computed with two variants of pressure-strain model with Reynolds-stress-transport closure (Craft [38]).

In the above context of discussing defects of the linear pressure-strain model, attention has been drawn to the role and the notional nature of the wall-related corrections (13). These terms had been formulated with specific reference to wall shear layers. When a flow impinges on the wall, as is the case close to the reattachment point of a separated shear layer, it turns out that $\Phi_{ij,2}$ produces entirely the opposite effect to that desired, i.e. $\Phi_{ij,2}$ *enhances* rather *inhibits* isotropisation. A manifestation of this defect emerges from Fig. 11. This shows results arising from the application of the standard Reynolds-stress closure to a sinusoidal pipe constriction (Lien & Leschziner [38]). The feature to focus on is the unrealistic angle of the separation streamline at reattachment. Very recently, Craft [39] has formulated a new wall-reflection model which is free from the above defect, and applied it to an impinging round jet. Lien and Leschziner [26] have also used the new model when predicting Driver & Seegmiller's backward-facing-step flow [27]. In both cases, the model has been observed to yield significant improvements.

As regards dissipation, no dramatic developments have taken place in recent years. In practice, dissipation is still represented by a single scale ε, although close to walls - where anisotropy rises rapidly, tensorial variants have been proposed. One is that of Launder & Reynolds [40],

$$\epsilon^{w}_{ij} = \frac{\epsilon}{k}\left(\overline{u_i u_j} + \overline{u_i u_k}\, n_k n_j + \overline{u_j u_k}\, n_k n_i + \delta_{ij}\, \overline{u_k u_\ell}\, n_k n_\ell\right) \Big/ \left[1 + \frac{5}{2}\, \frac{\overline{u_p u_q}\, n_p n_q}{k}\right] \quad (19)$$

Another, by Fu et al [36], blends the above with ε via,

$$\epsilon_{ij} = (1 - A^{0.5})\, \epsilon^{w}_{ij} + A^{0.5} \frac{2}{3} \delta_{ij}\, \epsilon \qquad (20)$$

The isotropic dissipation ε is still determined from a related transport equation of the type used within the k-ε modelling framework, although a number of variations have been put forward. Most have emerged in the course of devising the alternative non-linear pressure-strain models indicated above. The form used by Craft [39], for example, is:

$$\frac{d\epsilon}{dt} = \frac{\epsilon^2}{k} \left[- \frac{1.9}{(1 + 0.7A_2^{0.5}A)} + \frac{P}{\epsilon} \right] + d_\epsilon \qquad (21)$$

Clearly, the major novel element in this form is that the sink of ε is sensitized to anisotropy. It is also to be noted that the coefficient $C_{\varepsilon,1}$ multiplying P/ε [equation (10)] has been reduced from its standard value 1.44 to 1, the favourable consequence being that the influence of P/ε on ε is diminished.

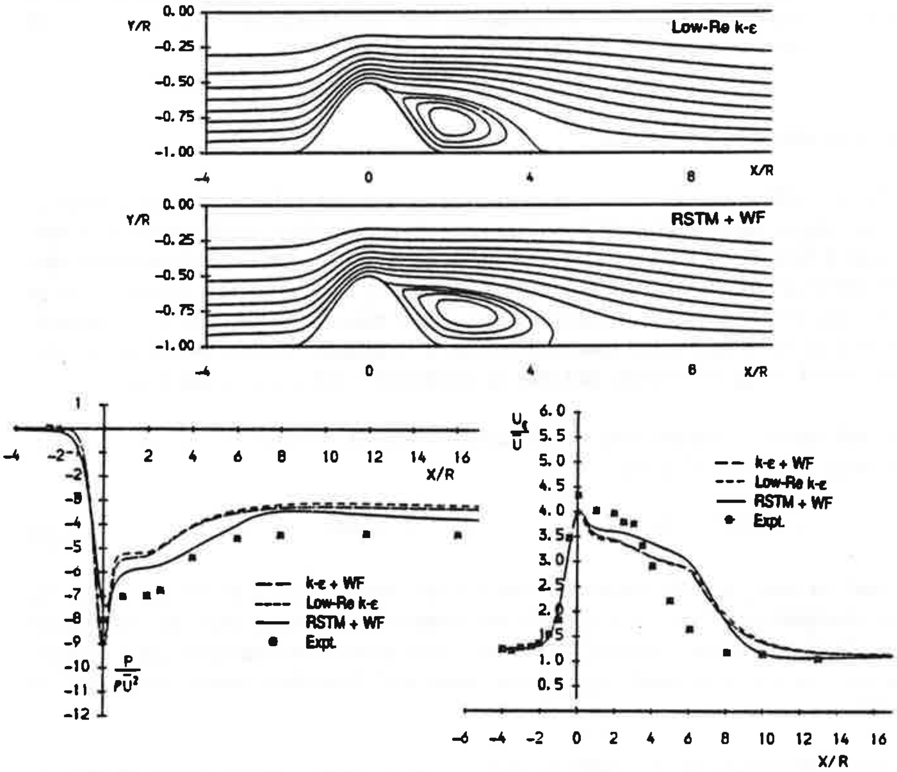

Fig. 11: Flow field, wall pressure and centre-line velocity variations in a sinusoidally constricted tube, computed with high-Re and low-Re eddy-viscosity and Reynolds-stress turbulence models (Lien and Leschziner [38])

A weakness of all forms of the dissipation equation is that they return an excessive near-wall length-scale value in non-equilibrium conditions resulting from adverse pressure gradients. Experiments show that the length scale $k^{3/2}/\varepsilon$ does not depart significantly from its equilibrium value 2.5y close to the wall, outside the viscous sub-layer. One consequence of this weakness is a seriously excessive level of wall heat transfer in flow recovering from separation and reattachment. This problem has been addressed, rather pragmatically, by Yap [41] who has added the following sink term to the ε-equation:

$$S_\epsilon = 0.83\left[\frac{k^{1.5}}{\ell_e \epsilon} - 1\right]\left[\frac{k^{1.5}}{\ell_e \epsilon}\right] \tag{22}$$

where ℓ_e is the equilibrium length scale 2.5y. It is readily recognised that this form increases ε in proportion to departures from the equilibrium value of ℓ_e, thus leading to a decrease in the length scale.

It is finally remarked that considerable efforts have also been made over the past three years to improve the 'standard' set of the flux-transport equations of Gibson & Launder [19] via non-linear approximations for the pressure/temperature-gradient terms, along routes analogous to those taken in designing the non-linear pressure-strain model for the stress equations. For details, see Craft [39].

Low-Reynolds-Number Effects

Low-Re modelling is little less than a quagmire, and this reflects a general lack of understanding of (and experimental evidence on) the mechanisms at play in the very thin near-wall region in which viscosity interacts with turbulence. It is only recently that direct numerical simulations, mainly at Stanford [42,43], have shed light on the variation of terms contributing to the balance of turbulence energy, stresses, and dissipation. These results have motivated renewed efforts to construct models which return the correct rate of decay of stresses and **rise** in dissipation very close to the wall .

Traditional models have emerged as extensions to high-Re variants, taking into account the limiting behaviour of k and ε,

$$k \rightarrow ay^2 + by^3 + \ldots \qquad \epsilon \rightarrow 2a + 4by + \ldots \tag{23}$$

as y tends to zero, and the constraint that viscous diffusion of k at the wall must be balance dissipation. This latter requirement immediately reveals that the dissipation must be finite at the wall. Indeed, direct numerical simulations indicate that ε reaches a maximum at the wall, implying that the usual wall boundary condition $\partial\varepsilon/\partial y=0$ is incorrect.

Some 15 different low-Re k-ε variants alone are in existence, and a review of most is provided by Patel et al [3]. The writer himself, working with Lien [44], has recently contributed to this plethora of models by formulating variants which satisfy length-scale constraints implied by the one-equation models of Wolfshtein [45] and Norris &

Reynolds [46] (see also Lien [47]). A recent model based on k and the turbulence vorticity ω has been proposed by Wilcox and his associates [48], and several one-equation models involving algebraic prescriptions of the length scale are reported in the literature (e.g. Wolfshtein [45], Norris & Reynolds [46], Davidson [49]).

Wall-induced attenuation of turbulence transport is modelled, almost without exception, via exponential decay functions pre-multiplying the eddy viscosity, and additional source terms in the ε-equation. These functions involve a turbulent Reynolds number of the form $k\ell/\nu$. In most models, ℓ is related explicitly to the wall distance, and this obviously restricts their application to near-wall regions. In contrast, the models of Jones & Launder [50] and Launder & Sharma [51] adopt the ratio $k^{3/2}/\varepsilon$ as the length scale, allowing application to low-shear (or slow), viscosity-dominated regions remote from walls. On the other hand, these same models tend, in certain circumstances, to suffer from stability problems near walls and require particularly high grid-line densities to ensure grid-independent solutions.

It is not the objective of this section to review the rationale and performance of established models. Rather, an indication is provided below of some fresh developments in this area. In view of the particular relevance of buoyancy-induced flow to room ventilation, it is instructive to give, prior to a consideration of recent efforts, one example of a particularly careful application of what appears to be the best conventional model to a buoyant cavity flow examined experimentally by Cheesewright and Ziai [52]. The application is that of Ince and Launder [2], using an extended variant of the Launder-Sharma k-ε model [51] (A similar study, adopting a somewhat less elaborate model variant is reported by Henkes [53]). The extension consists of including the buoyancy-generation terms into the k- and ε-equations, adding to the ε-equation Yap's length-scale correction and evaluating the heat fluxes from Daly & Harlow's [54] generalised gradient diffusion hypothesis,

$$\overline{u_i\theta} = - C_\theta \frac{k}{\varepsilon} \overline{u_i u_k} \frac{\partial \theta}{\partial x_\ell} \qquad (24)$$

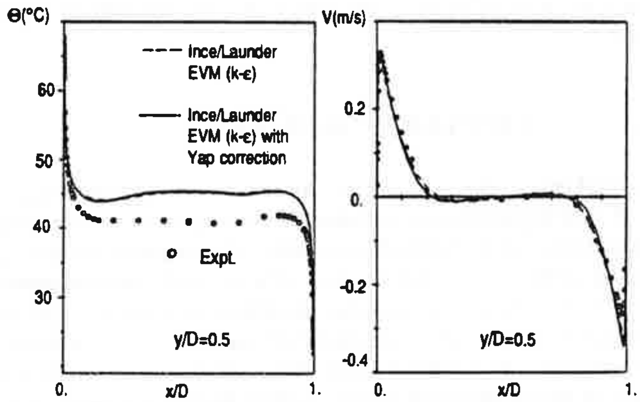

Fig. 12: Velocity and temperature profiles in buoyancy-driven flow in a 5:1 cavity at $Ra=5x10^{10}$ (Ince & Launder [2])

Use of the above tensorial flux model is of considerable importance to predictive accuracy, for it allows the large horizontal temperature gradient to influence the vertical flux, as is appropriate and clearly implied by the exact flux-generation terms in the flux-transport equations. Fig. 12 shows velocity and temperature distributions at one particular position across the cavity. As seen, predictive quality is good, indicating that this model is quite adequate for engineering purposes.

Recent fundamental efforts to improve low-Re models have followed three different routes: In the first, two-equation models are being formulated, again via functional correlation, but with reference to the aforementioned direct numerical simulations. Michelassi et al's model [55] is a good example of this rather pragmatic and somewhat opaque approach. The second route involves the introduction of exponential decay functions, very similar to those adopted in traditional k-ε models, into high-Re second-moment closures. the models of Launder & Shima [56] and Iacovides [6] fall into this category, the latter formulated specifically with a view to computing 3D curved-duct flows with strong transverse circulation. It must again be stressed here that this approach lacks physical realism, in so far as it attempts to capture the (inviscid) pressure-reflection process attenuating the wall-normal intensity via a viscosity-containing parameter. This fact is most clearly brought by applying the Gibson-Launder high-Re Reynolds-stress model [19] to a simple near-wall layer and noting that the shear stress emerges as $\overline{uv}=-0.26\overline{v^2}/\varepsilon(\partial U/\partial y)$. Low-Re k-$\varepsilon$ models adopt the form $\nu_t=f_\mu k^2/\varepsilon$, implying $f_\mu=2.9\overline{v^2}/k$, which agrees reasonably well with experiment. The most sophisticated approach, followed by Launder & Tselepidakis [7,59], involves the formulation of a non-linear pressure-strain model, within the framework of second-moment closure, which satisfies the aforementioned limiting constraints as turbulence approaches a two-dimensional state at the wall. It is only this approach which attempts to correctly mimic the reduction of viscous transport via the rapid decay of the wall-normal stress. Fig. 13 gives two results emerging from Launder & Tselepidakis' model. Fig. 13(a) contrasts predicted turbulence-intensity profiles with DNS calculations for a plane-channel flow, while Fig. 13(b) shows analogous profiles in a rotating channel, at a Rosby number of 0.05. In the latter, Coriolis forces interact with turbulence, a process resulting in a depression of turbulence on the duct's suction side and an amplification on the pressure side.

CONCLUDING REMARKS

The paper has highlighted some of the most influential issues contributing to the predictive realism of CFD algorithms for turbulent flows in general and separated flows in particular. Attention has been focused especially on turbulence modelling, within which recent developments in second-moment closure and low-Reynolds-number modelling have been reviewed. It is argued that modelling generality, in particular the correct sensitivity of solutions to extra strains and body forces require the use of second-moment-closure forms; that this argument finds ever widening acceptance is reflected by the increasing use of second-moment closure in high-technology areas such as aero-propulsion. The use of low-Reynolds-number modelling for near-wall regions is essential if wall heat transfer is to be captured correctly. This statement encompasses a range of non-equilibrium conditions such as free/mixed convection, reattachment and recovery therefrom and virtually all three-dimensional flows, whether attached or separated. Conventional two-equation models, whilst generally adequate, mis-represent the fundamental physical processes of wall-attenuated turbulence. Here again, second-moment closure is the lowest closure level offering scope for a correct representation, and current efforts have been highlighted.

The importance of adequate numerical resolution cannot be over-stated. Resource limitations seldom allow grid-independent solutions to be attained with first-order schemes, particularly in 3D conditions, and resort must be sought in higher-order schemes. These can present difficulties if applied to the turbulence equations, unless TVD-type formulations are employed.

Finally, because CFD involves highly non-linear and strongly interactive processes, some ill-understood, it is the writer's view that a high level of expertise, experience and insight will always be required to properly exploit the potential of CFD and, equally important, to appreciate its limitations. It is this which makes commercial CFD, unless entirely transparent, akin to 'fool's gold'.

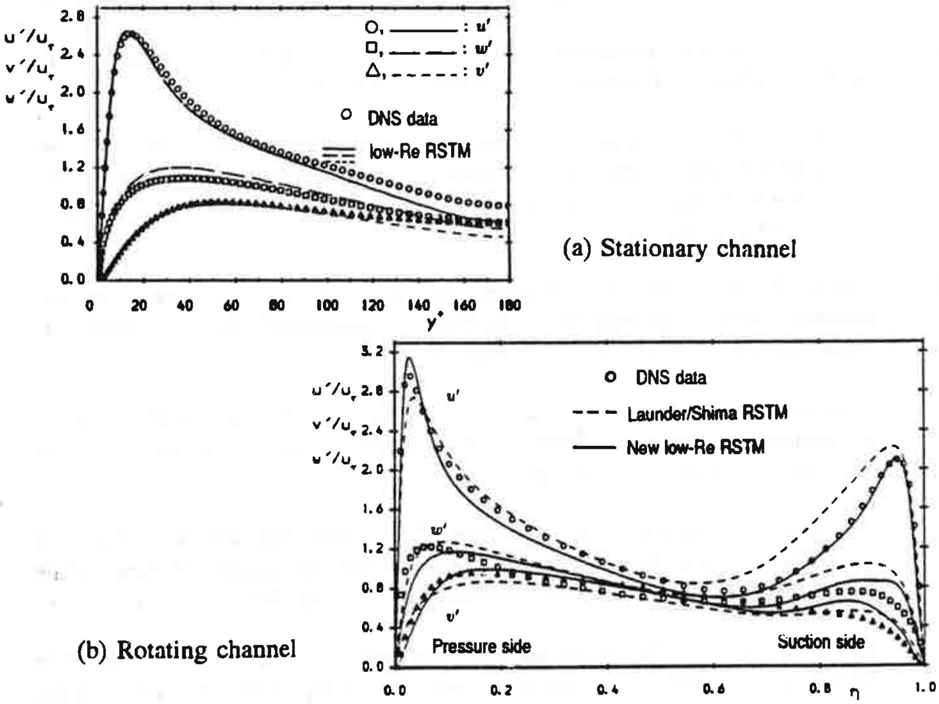

Fig. 13: Variations of turbulence intensity in stationary and rotating channels predicted with two low-Reynolds-number second-moment closures (Launder & Tselepidakis [7])

REFERENCES

[1] Kline, S.J., Reynolds, W.C. Schraub, F.A., **"The structure of turbulent boundary layers"** J.F.M., 1967, 30, p. 741

[2] Ince, N.Z. and Launder, B.E., **"On the computation of buoyancy-driven turbulent flows in rectangular enclosures"**, Int. J. Heat and Fluid Flow, 1989, 10, 2, pp. 110 - .

[4] Cotton, M. and Jackson, J.D., **"Calculation of turbulent mixed convection in a vertical tube using a low-Reynolds number k-ε turbulence model"**, Paper 9-6, Proc. 6th Turbulent Shear Flows Symp. Toulouse, 1987.

[5] Kawamura, H., **"Analysis of laminarization of heated turbulent gas using a two-equation model of turbulence"**, Proc. wind Symp. on turbulent Shear Flows, London, 1979.

[6] Iacovides, H., **"An ASM closure for the low-Re sublayer"** Proc. 5th UMIST CFD Colloquium, Mech. Eng. Dept. Thermofluids Division, Manchester, 1992.

[7] Launder, B.E. and Tselepidakis, D.P., **"Contribution to the modelling of near-wall turbulence"**, Turbulent Shear Flows-8, Springer Verlag, 1992.

[8] Lin. C.A., **"Three-dimensional computations of transient interaction between radially injected jet and swirling cross-flow using second-moment closure"**, Proc. 4th Int. Symp. on Computational Fluid Dynamics, University of California, Davis, 1991, pp. 687-691.

[9] Franke, R., Rodi, W. and Schoenung, B., **"Analysis of experimental vortex-shedding data with respect to turbulence modelling"**, Proc.7th Symp. on Turbulent Shear Flows, Stanford, 1989, pp. 24.4.1-24.4.6.

[10] Tamura, T., Ohta, I. and Kuwahara, K., **"On the reliability of two-dimensional simulation for unsteady flows around a cylinder-type structure"**, J. Wind Eng. Ind. Aerodyn., 35, 1990, pp. 275-298.

[11] Murakami, S., Mochida, A. and Hibi, K., **"Three-dimensional numerical simulation of air flow around a cubic model by means of large eddy simulation"**, J. Wind Eng. Ind. Aerodyn., 25, 1985 pp. 291-305

[12] Reynolds, W.C., **"The potential and limitations of direct and large-eddy simulations"**, in Wither Turbulence? Turbulence at the Crossroads, J.L. Lumley (ed.), Springer, 1990, pp. 313-343.

[13] Raithby, G.D., **"Skew upwind differencing schemes for problems involving fluid flow"**, Comp. Meths. Appl. Mech. Eng., 1976, 9, pp. 153.

[14] Leonard, B.P., "**A stable and accurate convective modelling procedure based on quadratic upstream-weighted interpolation**", Comp. Meths. Appl. Mech. Eng., 1979, pp. 59-98.

[15] Davidson, L., "**Numerical simulation of turbulent flow in ventilated rooms**", PhD Thesis, Chalmers University of Technology, Goteborg, 1989.

[16] Nasser, A.G., "**Compact finite-difference finite-volume schemes for unsteady recirculating flows**", Ph.D. Thesis, University of Manchester, 1990.

[17] Launder, B.E., "**Second-moment closure: present and future, Int. J. Heat and Fluid Flow**", 1989, 10, pp. 282-300.

[18] Leschziner, M.A., "**Modelling engineering flows with Reynolds-stress turbulence closure**", J. Wind Eng. Ind. Aerodyn., 1990, 35, pp. 21-47.

[19] M.M. Gibson and B.E. Launder, "**Ground effects on pressure fluctuations in the atmospheric boundary layer**", J. Fluid Mech, 1978, Vol. 86, pp. 491-511.

[20] B.E. Launder, G. Reece and W. Rodi, W., "**Progress in the development of a Reynolds stress turbulence closure**", J. Fluid Mech., 1975, Vol. 68, pp. 537-566.

[21] W. Rodi, "**A new algebraic relation for calculating the Reynolds stresses**", ZAMM, 1976, 56, p. 219.

[22] S. Fu, P.G. Huang, B.E. Launder and M.A. Leschziner, M.A., "**A comparison of algebraic and differential second-moment closures with and without swirl**", ASME J. Fluids Eng., 1988. Vol 110, pp. 216-221.

[23] D.R. Boyle and M.W. Golay, "**Measurement of a recirculating two-dimensional flow and comparison to turbulence model prediction. I: Steady state case**", ASME J. Fluids Eng, 1982, Vol. 105, pp. 446-454.

[24] P.G. Huang and M.A. Leschziner, M.A., "**Stabilization of recirculating flow computations performed with second-moment closure and third-order discretization**", Proc. 5th Symp. on Turbulent Shear Flows, Cornell University, 1985, pp. 20.7-21.2.

[25] Leschziner, M.A., Kadja,M. and Lea, C.J., "**A combined computational and experimental study of separated flow in an expanding annular passage**", in Refined flow modelling and Turbulence Measurements, Y. Iwasa, N. Tamai and A. Wada (eds.), Universal Academic Press, 1988, pp. 129-138.

[26] Lien, F.S. and Leschziner, M.A., Unpublished results contributed to 1991/92 Stanford Trials (P. Bradshaw), Stanford University, 1992.

[27] Driver, D.M. and Seegmiller, H.L., "**Feature of a reattaching turbulent shear layer subject to an adverse pressure gradient**", AIAA J., 1985, 23, pp. 163-171.

[28] Saripalli, K.R., Turbulent Shear Flows 5, (F. Durst, B.E. Launder, F.W. White and J.H. Whitelaw eds.), Springer, 1987, pp. 146-168.

[29] Ince, N.Z. and Leschziner, M.A., "**Second-moment modelling of incompressible impinging twin jets**", Proc. 5th UMIST CFD Colloquium, Dept. of Mech. Eng., Thermofluids Division, 1992.

[30] Leschziner, M.A., "**Numerical prediction of the internal density jump**", Proc. XVIII IAHR Congress, Calgary, 1979, 3, pp. 33-40.

[31] McGuirk, J.J. and Papadimitriou, C., "**Buoyant surface layers under fully entraining and internal hydraulic jump conditions**", Proc. 5th Int. Symp. on Turbulent Shear Flows, Cornell University, 1985, pp. 22.33-22.41.

[32] Viollet, P.-L, "**Turbulent mixing in a two-layer stratified shear flow**", Second Int. Symp. on Stratified Flows, Trondheim, 1980, pp. 315-325.

[33] McGuirk, J.J., and Rodi, W., "**Mathematical modelling of three-dimensional heated surface jets**", JFM, 1979, 95, p. 609.

[34] Leschziner, M.A. and Rodi, W, "**Calculation of a heated water discharge**", ASCE J. of Hydraulic Engineering, 1983, 109, pp. 1380-1384.

[35] Shih, P.H. and Lumley, J.L., "**Modelling of pressure correlation terms in Reynolds-stress and scalar flux equations**", Rept. FDA-85-3, Sibley School of Mech. and Aerospace Eng., Cornell, 1985.

[36] Fu, S., Launder, B.E. and Tselepidakis, D.P., "**Accommodating the effects of high strain rates in modelling the pressure-strain correlation**", Report TFD/87/5, UMIST, Dept. Mech. Engng., Thermofluids Div., 1987.

[37] Craft, T.J. and Launder, B.E., "**A new model of wall-reflection effects on the pressure-strain correlation and its application to the turbulent impinging jet**", AIAA J., To appear 1992.

[38] Lien, F.S. and Leschziner, M.A., "**Second-moment modelling of recirculating flow with a non-orthogonal collocated finite-volume algorithm**", Proc. 8th Symp. on Turbulent Shear Flows, Munich, Sept 1991, pp. 20.5.1 - 20.5.6. (To be published in hard-cover by Springer Verlag).

[39] Craft, T.J., "**Second-moment modelling of turbulent scalar transport**", PhD Thesis, University of Manchester, Institute of Science and Technology, 1991.

[40] Launder, B.E. and Reynolds, W.C., **"Asymptotic near-wall stress distribution rates in turbulent flow", Physics Fluids, 1983, 26, pp. 1157-1158.**

[41] Yap, C.R., **"Turbulent heat and momentum transfer in recirculating and impinging flows"**, Ph.D. Thesis, Faculty of Technology, University of Manchester, 1987.

[42] Mansour, N.N., Kim, J. and Moin, P., **"Near-wall k-ε turbulence modelling"**, Proc. 6th Symp. on Turbulent Shear Flows, Toulouse, France, 1987.

[43] Kim, J., Moin, P. and Moser, R., **"Turbulence statistics in fully developed channel flow at low Reynolds number"**, J. Fluid Mech., 177, pp. 123-166.

[44] Lien, F.S., Leschziner, M.A., **"Modelling variable-area curved duct flow with a 3D non-orthogonal collocated FV method"**, Proc. 4th UMIST CFD Colloquium, Dept. of Mech. Eng., Thermofluids Division, 1990.

[45] Wolfshtein, M.W., **"The velocity and temperature distribution in one-dimensional flow with turbulence augmentation and pressure gradient"**, Int. J. Heat Mass Transfer, 1969, 12, p. 301.

[46] Norris, L.H. and Reynolds, W.C., **"Turbulent channel flow with a moving wavy boundary"**, Rep. FM-10, Dept. of Mech. Engrg., Stanford University, 1975.

[47] Lien, F.S., **"Computational modelling of 3D flow in complex ducts and passages"**, PhD Thesis, University of Manchester, 1992.

[48] Wilcox, D.C., **"Reassessment of the scale-determining equation for advanced turbulence models"**, AIAA J., 1988, 26, pp. 1299-1310.

[49] Davidson, L., and Olsson, E., **"Calculation of some parabolic and elliptic flows using a new one-equation turbulence model"**, Proc. 5th Int. Conf. on Numerical Methods in Laminar and Turbulent Flow, Montreal, 1987, 1, pp. 411-422.

[50] Jones, W.P. and Launder, B.E., **"The prediction of laminarisation with a two-equation model of turbulence"**, Int. J. Heat Mass Transfer, 1972, 15, pp. 301-314.

[51] Launder, B.E. and Sharma, B.I., **"Application of the energy dissipation model of turbulence to the calculation of flow near a spinning disc"**, Lett Heat Mass Transfer, 1974, 2, p. 1.

[52] Cheesewright, R. and Ziai, S., **"Distributions of temperature and local heat transfer rate in turbulent natural convection in a large cavity"**, Paper NS-03, Proc. 8th Int. Heat Transfer Conf., San Francisco, 1986.

[53] Henkes. R.A.W.M. "**Natural-convection boundary layers**", PhD Thesis, University of Delft, 1990.

[54] Daly, B.J. and Harlow, F.H., "**Transport equations of turbulence**", Phys. Fluids, 1970, Vol. 13, pp. 2634-2649.

[55] Michelassi, V., Rodi, W. and Scheuerer, G., "**Testing a low-Reynolds number k~ε turbulence model based on direct simulation data**", paper presented at 8th Symp. on Turbulent Shear Flows, Munich, 1990.

[56] Launder, B.E. and Shima, N., "**A second-moment closure for the near-wall sublayer**", AIAA J., 1989, 127, pp. 1319-1325.

[57] Leschziner, M.A., "Practical evaluation of three finite difference schemes for the computation of steady-state recirculating flows", Comp. Meths. Appl. Mech. Engg., 1980, 23, pp. 293-312.

[58] Cresswell, R., Haroutunian, V., Ince, N.Z., Launder, B.E. and Szczepura R.T., "Measurement and modelling of buoyancy-modified, elliptic turbulent shear flows", Proc. 7th Symp. on Turbulent Shear Flows, Stanford University, 1989, pp. 12.4.1-12.4.6.

[59] Launder, B.E. and Tselepidakis, D.T., "Applicationof a new second moment closure to the prediction of flow in a rotating plane channel",to be published, 1992.